HONGXING LIU
CHANGLONG WANG
LIE CHEN
SHICHANG LIU
and
JIAN YANG

Preparation and properties of autoclaved sand-bricks using iron ore tailings and waste rock

This study focuses on autoclaving reaction activity of hornblende, biotite and albite, the influences of the compositional characteristics, ingredients and forming, autoclaving processes and the properties of autoclaved sand-lime brick from iron ore tailings and waste rock. The results are shown as follows: under autoclaving 12 h hydrothermal conditions at 185ºC and 1.25 MPa, albite has autoclaving reaction activity while hornblednde and biotite do not have; autoclaving hydration products in albite system contain hibschite and tobermorite; the optimal proportion of major raw materials meeting with the technical requirements of GB11945—1999 for MU15 sand-lime bricks is as follows: iron ore tailings 75%, waste rock 13% and lime 12%; XRD and FE-SEM analyses show that the newly generated crystalline phases in the sand-lime brick samples are tobermorite, hibschite, C-S-H gels, quartz and residual minerals from iron ore tailings.

Keywords: *autoclaving reaction activity, iron ore tailings, waste rock, autoclaved sand-lime brick, tobermorit*

1. Introduction

Iron ore tailings (IOT) are usually left untreated in China. With the rapid development of iron and steel industry and iron ore mining, the accumulation of IOT in the tailing pond is rising steadily [1]. Since the untreated IOT can cause environmental pollution and its storage requires large space and heavy investment, reasonable utilization of IOT has become a major concern [2-3]. In China, IOT is mainly used for extraction of valuable elements [3], making building materials [4-8] or filling materials [9-11]. Zhang [12] and Jia et al. [13] prepared autoclaved bricks using IOT, cement, gypsum and fly ash, in which the maximum doping amount of IOT reached 65%. Zhao et al. [14,15] prepared autoclaved bricks using hematite tailings, yellow sand and lime, in which the maximum doping amount of tailings reached 70%. At present, the utilization rate of IOT remains low and the technology of preparing autoclaved bricks from IOT is not fully described or popularized. In this study, tailings from magnetite quartzite-type iron ores mined at Dashihe by Shougang Mining Company were used. Besides quartz, three other SiO_2-containing minerals in the tailings, hornblende, biotite and albite, were characterized during autoclaving experiment under hydrothermal conditions using IOT, waste rock (WR) and lime as raw materials. The reactivity of the three minerals was tested by preparing bricks from a single mineral and lime. The purpose was to increase the doping amount and utilization rate of IOT. Microscopic performance and strength forming mechanism of the autoclaved bricks were characterized by using X-ray diffraction analysis (XRD), scanning electron microscope (SEM), and an explanation was provided for the strength forming mechanism.

Messrs. Hongxing Liu, Changlong Wang, Lie Chen, Shichang Liu and Jian Yang, State Key Laboratory of High-Efficient Mining and Safety of Metal Mines, University of Science and Technology Beijing, Beijing 100083, China, School of Resources and Environmental Engineering, Jiangxi University of Science and Technology , Ganzhou Jiangxi Province, 341000, China, School of Civil Engineering, Hebei University of Engineering, Handan Hebei Province, 056038, China, Email: lhx-lhx971@163.com; 13716996653@139.com

2. Materials and methods

2.1 Experimental materials

The raw materials and their mass fractions are shown in Tab. 1. The reactivity of hornblende, biotite and albite in autoclaving reaction was determined, with the degree of fineness controlled below 0.08mm. The tailings used were from Qian'an Dashihe Deposit mined by Shougang Mining Company. The major minerals of IOT included: quartz, hornblende, biotite, albite and a few amount of chlorite, calcite and hematite. To save the use amount of quicklime and to ensure the forming of the autoclaved bricks, WR was added into the quicklime cementing agent. WR was obtained by mechanical comminution of stripped rocks from the Deposit, with particle size of 3-8 mm and bulk density of 1.43×10^3 kg m^{-3}. As to the degree of fineness, less than 15% of quicklime remained after passing through the 0.08mm square-mesh sieve. The effective content of CaO was 67.2%, with digestion time of 8 min and digestion temperature of 68 ºC.

2.2 Experimental Method

2.2.1 Preparation of specimens using a single mineral and lime

Three minerals were mixed with lime at the fraction of 2:1, respectively, and then added with water and stirred properly.

TABLE 1 CHEMICAL COMPOSITION OF RAW MATERIALS (WT.%)

Material	SiO_2	Al_2O_3	FeO	Fe_2O_3	CaO	MgO	Na_2O	K_2O	LOI
Iron ore tailings	72.48	7.37	1.19	6.08	2.78	3.59	0.98	2.11	2.73
Waste rock	68.65	9.26	0.90	5.85	3.50	3.11	0.62	2.60	2.04
Lime	6.63	4.85	2.48	4.53	70.46	3.63	0.63	1.25	5.13
Hornblende	52.88	14.36	11.69	1.68	0.54	15.70	0.20	—	2.10
Biotite	35.70	11.68	11.00	6.44	6.21	12.28	—	6.37	2.54
Albite	66.10	20.40	0.06	0.06	1.86	9.50	9.50	0.90	0.31

TABLE 2 PARTICLE SIZE DISTRIBUTION OF IRON ORE TAILINGS

Sieve Size/mm	+1.25	-1.25 +0.63	-0.63 +0.32	-0.32 +0.16	-0.16 +0.08	-0.08
Meter sieve/%	1.7	6.1	6.7	36.1	41.3	8.1
Cumulative sieve/%		7.8	14.5	72.2	82.6	

The slurries of the three minerals were poured into Φ50 mm×50 mm polyvinyl chloride cylindrical container, which was covered with a ventilated lid. The slurries first stood at room temperature for 12h and were then transferred to the autoclave for autoclaving reaction at increasing temperature and increasing pressure for 2h, constant temperature and constant pressure for 8h (1.25 MPa, 185ºC) and decreasing tempreautre and decreasing pressure for 2 h.

2.2.2 Preparation of autoclaved bricks using IOT

IOT, ground quicklime and WR were mixed with 10% water and subjected to intense stirring, so that the sand particles were evenly enveloped by calcium hydroxide particles. After that, the slurry stood for 2h and was again mixed with 5% water.

The slurry was made into 240 mm×115 mm×53 mm adobe bricks with forming pressure of 20 KN and cured for 3h. Then autoclaving reaction was conducted at increasing temperature for 2h, constant pressure for 8h (highest pressure 1.25 MPa and highest temperature 185ºC), and decreasing temperature for 2h. Finally the bricks were cooled before being taken out.

2.2.3 Sample characterization

Rigaku D/max-RC diffractometer (12 kW, Cu target, wavelength 1.5406 nm, working current 150 mA, working voltage 40 kV) was used for phase determination of the prepared specimens. SUPRAtm55 field emission scanning electron (FE-SEM) was used to observe the microscopic morphology of the hydration products in the autoclaved bricks.

The mechanical properties of the specimens were determined according to Chinese standard for autoclaved lime-sand bricks (GB 11945-1999) and GB/T 2542-2003 Test methods for wall bricks.

3. Result and discussion

3.1 REACTIVITY OF A SINGLE MINERAL IN AUTOCLAVING REACTION

Fig.1 shows the XRD spectra of the specimens prepared using hornblende, biotite, albite and lime under hydrothermal conditions of 185ºC and 1.25 MPa saturated vapor pressure for 12h, respectively. It can be seen from Fig.1(a) that the major minerals in the specimen prepared from hornblende were hornblende, $Ca(OH)_2$ and $CaCO_3$, without the formation of autoclaved products. It can be inferred that under the above hydrothermal conditions, hornblende did not react with $Ca(OH)_2$. Fig.1(b) is the specimen prepared from biotite, in which no autoclaved products were detected either and the major minerals were biotite, $Ca(OH)_2$ and $CaCO_3$. Hornblende is a monoclinic double-chain silicate, in which the M1, M2 and M3 sites of the $[SiO_4]$ chain are occupied by cations with small radius such as Mg^{2+}, Fe^{2+} and Fe^{3+}. Ca^{2+} ions with large radius cannot enter the lattice to cause depolymerization along with OH^- ions. Biotite comprises TOT layers containing mainly Mg, Ti and Fe, bonded by interstitial K atoms. The Mg^{2+} and Fe^{2+} in the O layer constitute the $[M(O,OH)_6]$ octahedral layer with the non-bridged O and OH in the T layer. Therefore, the Ca^{2+} ions cannot enter the O layer to cause depolymerization of the TOT layers along with OH^- ions. Instead Ca^{2+} ions only enter the interlayers and undergo ion exchange with K^+ ions. That is why hornblende and biotite have no hydrothermal reactivity.

Fig.1(c) is the XRD spectrum of the specimen prepared from albite, indicating obvious reduction in intensity of diffraction peak of $Ca(OH)_2$. In the specimen, a large amount of hydration products such as tobermorite and hibschite were detected. Albite is a framework silicate occupied by Na^+ ions with large radius. Therefore, Ca^{2+} and OH^- ions can enter the lattice framework. The OH^- ions first open the Si(Al)-O-Si structure, forming isolated $[Si(Al)(O,OH)_4]$ [16,17]. The Na^+ ions occupying the holes of albite undergo ion exchange with the hydrated Ca^{2+} ions rather than with H^+ ions [18]. As a result, depolymerization and hydration of the albite occur, with the formation of new silicate phases.

Hibschite is a calcium- and aluminum-containing hydrogarnet. The content of Al in the raw material is directly proportional to the generated amount of hibschite [19] and albite has a high content of Al (Al_2O_3 20.40%). Therefore, hibschite is the first silicate phase produced by autoclaving reaction using the CaO-Al_2O_3-SiO_2-H_2O system. As the $[OH^-]$ in the pore solution decreased over time, hibschite was transformed into more stable aluminum-containing silicate phase, such as tobermorite [20]. At the beginning, $Ca(OH)_2$

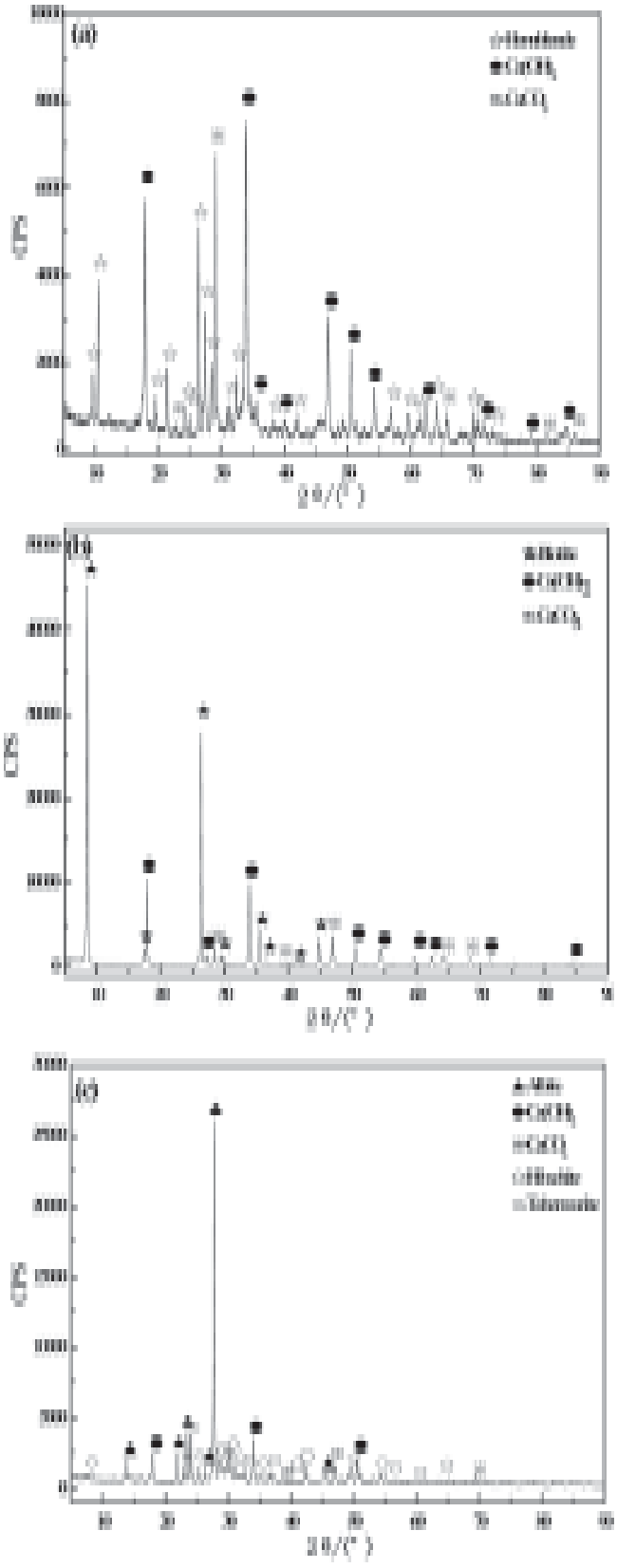

Fig.1 XRD patterns of hornblende, biotite and albite $Ca(OH)_2$ system in autoclaving condition
(a: hornblende, b:biotite, c: albite)

reacted violently with albite with a few silicon and aluminum dissolved out from the albite. Therefore, insufficient $A1^{3+}$ and Si^{4+} ions were available for the hydration and hibschite was formed in large quantity with a high degree of crystallization. As more $A1^{3+}$ and Si^{4+} ions were supplied over time, the initially alkaline environment was changed, and the dissolution of the hibschite was accelerated. The Ca^{2+} ions from the hibschite reacted with the newly dissolved $A1^{3+}$ and Si^{4+} ions, giving rise to tobermorite. But due to limited time, hibschite was not completely transformed into tobermorite, resulting in the coexistence of the two minerals in the products.

3.2 Effect of doping amount of IOT on the mechanical performance of the autoclaved bricks

The amount of quicklime was fixed at 12% of total mass of the dry materials, while the doping amount of IOT and WR was changed. For the doping amount of IOT was 55%, 60%, 65%, 70%, 75%, 80% and 85%, the autoclaved bricks were designated as T1, T2, T3, T4, T5, T6 and T7, respectively. Fig.2 shows the effect of doping amount of IOT on the mechanical properties of the autoclaved bricks when the sand-lime bricks were cooled to below 40ºC in the autoclave.

The amount of IOT as the siliceous material and that of quicklime as the calcareous material plays a crucial role in the mechanical properties of the autoclaved bricks. SiO_2, the main ingredient in IOT, has reactivity in autoclaving reaction and undergoes a series of physical and chemical changes with quicklime to form the autoclaved bricks [21]. With the amount of quicklime fixed, the doping amount of IOT was changed to observe its impact on the strength of the autoclaved bricks.

As shown in Fig.2, as the amount of IOT increased and the amount of WR decreased, the compressive strength and flexural strength of the autoclaved bricks first increased and then decreased. Specimen T5 achieved the highest

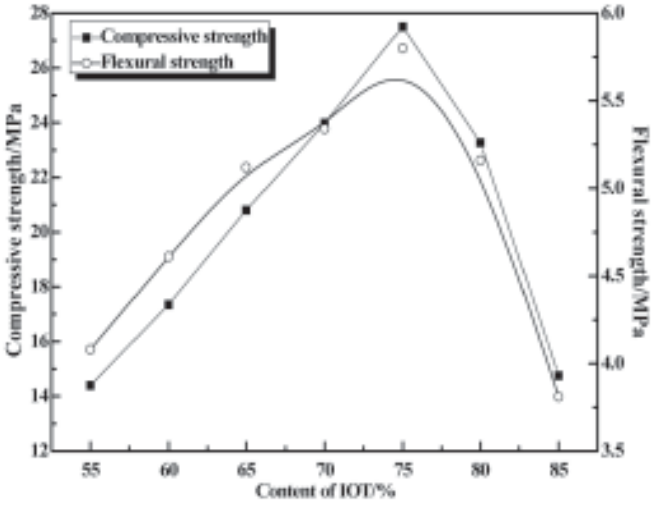

Fig.2 The influence of IOT content on the mechanical properties of autoclaved sand-lime bricks

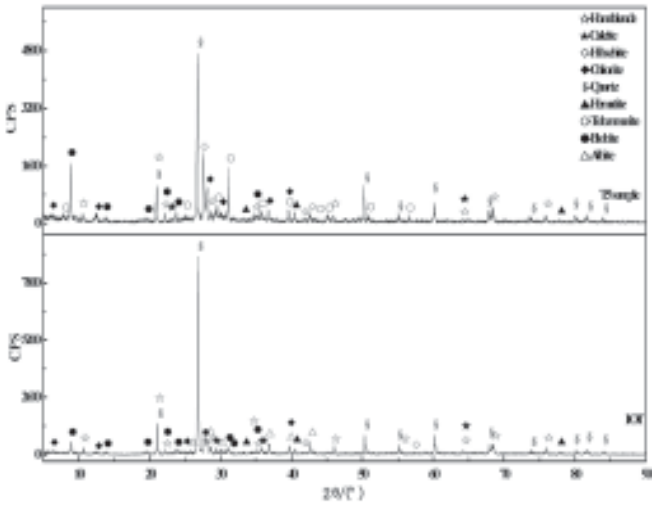

Fig.3 XRD spectra of IOT and T5 sample

compressive strength (27.49 MPa) and the highest flexural strength (5.82 MPa) when the doping amount of IOT was 75%. As shown in Table 1, the content of CaO and MgO in the quicklime was only 74.09%, which did not meet the JC/T 479-92 standard for quicklime, though high strength was achieved in the specimen. This is because of the high content of clay minerals in the quicklime. The calcined clay minerals had higher reactivity and reacted with lime to produce autoclaved bricks with higher strength [22].

Although the content of SiO_2 in free state increases with the increasing doping amount of IOT and SiO_2 reacts slowly with CaO under room temperature, they can react to produce high-strength products by autoclaving reaction under 1.25 MPa and 185ºC. When the doping amount of IOT was low and that of WR was high, the strength of the autoclaved bricks was low. This is probably due to the high amount of unreacted $Ca(OH)_2$ and small amount of hydration products. The hydration products are first formed on the particle surface, and as the time of pressurization increases, the thickness of the hydration product layer increases and the hydration products will go into the spaces between the particles. When the doping amount of IOT was very low, the amount of hydration products formed was insufficient to envelop the particles of IOT and WR, resulting in low strength. But when the doping amount of IOT was too high, the small particles of IOT would fill up the spaces of the autoclaved bricks, making the bricks too compact. Therefore, the hydration products formed on the particle surface could not go into the spaces between the particles, also resulting in low strength.

Thus the mechanical properties of specimen T5 prepared at 75% IOT and 13% WR met the requirement for MU15 sand-lime bricks in GB 11945-1999 standard. This proportion was determined as the optimal.

3.3 Composition and morphology of the autoclaved bricks

Phase composition of specimen T5 and IOT was compared using X-ray diffraction, with the results shown in Fig.3. Four major differences were observed from XRD spectra of the two. First, the characteristic peaks of quartz in IOT were weakened, indicating reduced content of quartz after autoclaving reaction. Second, characteristic peaks of tobermorite and hibschite appeared in specimen T5. Third, characteristic peak of albite was absent for specimen T5. Fourth, 2è in the XRD spectra of specimen T5 was the wide concave hull background under 26-34° diffraction peak.

After autoclaving reaction, hydrated phases such as calcium silicate hydrated (C-S-H) and tobermorite were formed, which had a large impact on the mechanical performance of the autoclaved bricks [21]. As SiO_2 was constantly dissolved out from the IOT and reacted with $Ca(OH)_2$ to form tobermorite and hibschite, the diffraction peak of quartz in the product was weakened, indicating the hydration between quartz and $Ca(OH)_2$. The residual quartz acted as the aggregates. The disappearance of diffraction peak of albite in specimen T5 indicated the consumption of albite with the formation of tobermorite and hibschite. Albite

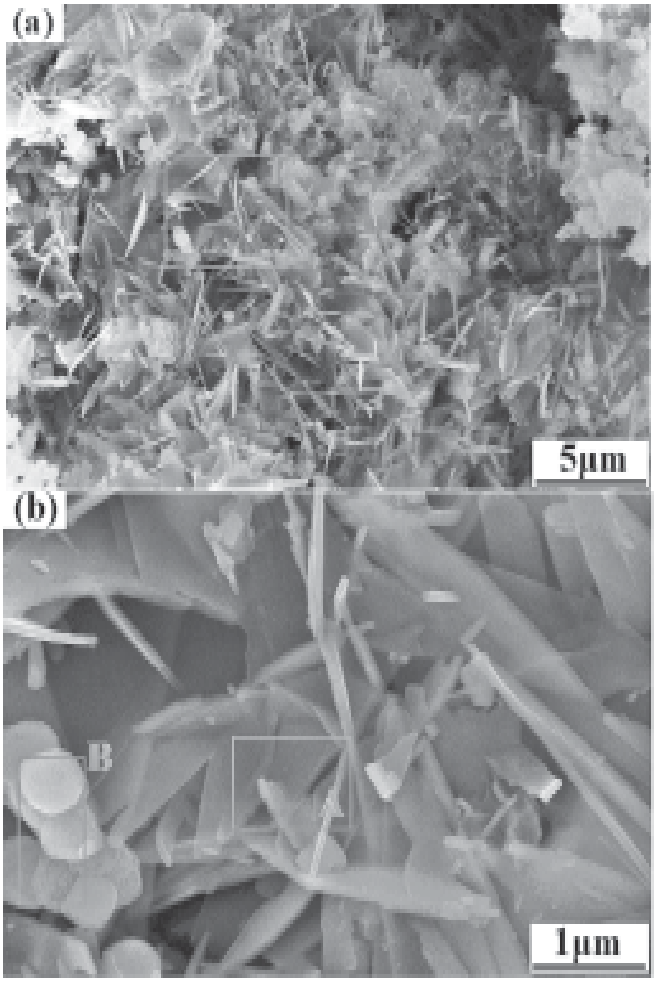

Fig.4 FE-SEM micrographs of hydrated products of T5 sample (a)microstructure of hydrated products of T5 sample; (b) high magnification view of the markted region 1 in (a)

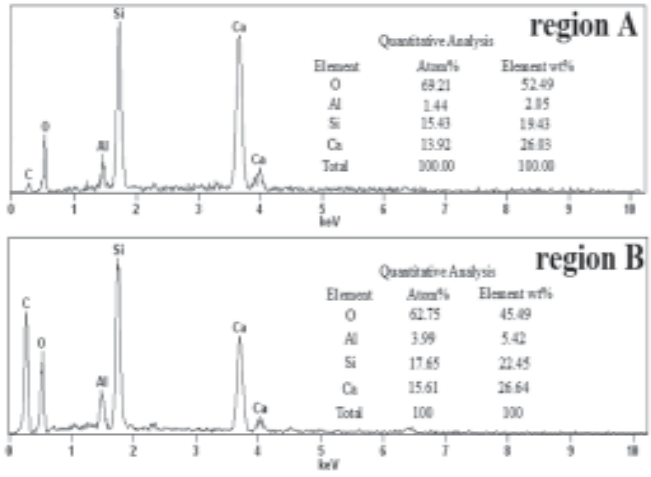

Fig.5 The EDX spectra of marked region A and B in the Fig.4(b)

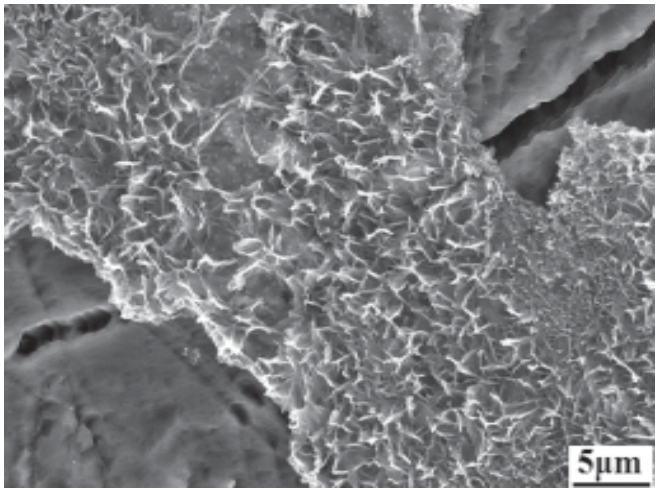

Fig.6 Binding state of hydrate product and waste rock particle

had reactivity in autoclaving reaction, In Fig.3, 2θ was the wide concave hull background under 26-34° diffraction peak, indicating the presence of amorphous substances or low crystallinity substances (without diffraction peaks) in the specimen. This led to widening of the diffraction peaks and affected the background value of XRD spectra [23].

Fig.4 shows the FE-SEM images of the autoclaved bricks after autoclaving reaction for 12h. In Fig.4(a), a large amount of hydration products appeared, typically the flake-like tobermorite crystals and C-S-H gel with low crystallinity. Spherical hibschite particles are scattered in the specimen, and the hibschite particles aggregated together occasionally. Tobermorite crystals were intercalated with C-S-H gel, making the structure more compact and increasing the compressive strength of the autoclaved bricks. Fig. (b) is the magnified version of the marked region in (a). This area contains a large amount of flake-like tobermorite crystals with high crystallinity and thickness of 0.1-0.3 μm. In the lower left corner are similar to the grapes or spherical contour hibschite, and its diameter of the single particle is about 0.3-0.5 μm.

The EDX spectra in region A and B in Fig.4(b) were analyzed (Fig.5). The presence of Al in the hydration products can be explained by the presence of Al in IOT. Some [SiO_4] tetrahedrons were replaced by [AlO_4] tetrahedrons. In region A, nCa/n(Si+Al) = 0.25 for the hydration product, which was consistent with n(Ca)/n(Si) = 0.83 for tobermorite ($Ca_5(OH)_2Si_6O_{16}$!$4H_2O$). In region B, nCa/n(Si+Al) = 0.721 for the hydration product, which was consistent with n(Ca)/n(Si+Al)=0.721 for hibschite ($Al_2Ca_3(SiO_4)_{2.16}(OH)_{3.36}$).

Fig. 6 shows SEM photos of WR particles and the surrounding products in specimen T5. As seen from Fig. 6, the tobermorite crystals adhered to the surface of WR particles, bridging the space of two particles. This increased the strength of the specimen.

4. Conclusions

Under the hydrothermal conditions of 1.25 MPa and 185ºC, albite showed reactivity and tobermorite and hibschite were formed. In contrast, hornblende and biotite had no such reactivity.

Autoclaved bricks that met the requirements for MU15 sand-lime bricks in Chinese standard for autoclaved lime-sand bricks (GB 11945-1999) were prepared using IOT and WR from Dashihe Deposit. The optimal process parameters were determined as follows: mass ratio of IOT, WR and quicklime = 75:13:12. The slurry was stirred twice and the 15% of water was added. Autoclaving reaction was carried out under the following conditions: increasing temperature and increasing pressure for 2h, constant temperature and constant pressure for 8h (pressure 1.25 MPa, temperature 185ºC), decreasing temperature and decreasing pressure for 2h.

XRD and SEM characterization indicated that a large amount of flake-like tobermorite crystals, amorphous or low crystallinity C-S-H, and spherical aggregates of hibschite particles were formed in the autoclaved bricks.

Acknowledgements

The authors gratefully acknowledge financial support from the National Key Technology R&D Program (2014BAE05B00), China Postdoctoral Science Foundation (2015T80095, 2015M580106), Natural Science Foundation of Hebei Province (E2015402057), supported by State Key Laboratory of Solid Waste Reuse for Building Materials (SWR-2014-007), supported by science and technology research project of higher education universities in Hebei Province (ZD2016014), supported by Comprehensive Utilization of Tailing Resources Key Laboratory of Shaanxi Province (2014SKY-WK010), Construction Science and Technology Foundation of Hebei Province (2012-136).

References

[1] Zhang S., Xue X., Liu X., Duan P., Yang H., Jiang T.,

Wang D., Liu R. (2006): Current situation and comprehensive utilization of iron ore tailing resources. Journal of Mining Science, 42(4): 403-408.

[2] Yao M. G., Wang J. L., Ren R. C. (2011): Study and comprehensive utilization of iron ore tailings resources in the western Liaoning Province. Mining Engineering, 9(4): 53-56.

[3] C. L, H. Sun H., Bai J., Li L. T. (2010): Innovative methodology for comprehensive utilization of iron ore tailings: Part 1. The recovery of iron from iron ore tailings using magnetic separation after magnetizing roasting. Journal of Hazardous Materials, 174(1-3): 71-77.

[4] Wang C. L., Ni W., Qiao C. Y., Wang S., Wu H., Li Y. (2013): Preparation and properties of autoclaved aerated concrete using iron ore tailings. chinese Journal of Materials Research, vol. 27(2): 157-162.

[5] Yi Z.L., Sun H. H., Li C., Sun Y. M., Li Y. (2010): Relationship between polymerization degree and cementitious activity of iron ore tailing. International Journal of Minerals, Metallurgy, and Materials, 17 (1): 116-122.

[6] Li C., Sun H. H., Yi Z. L., Li L. T. (2010): Innovative methodology for comprehensive utilization of iron ore tailings: Part 2: The residues after iron recovery from iron ore tailings to prepare cementitious material. Journal of Hazardous Materials, 174(1-3): 78-83.

[7] Yi Z. L., Sun H. H., Wei X. Q., Li C. (2009): Iron ore tailings used for the preparation of cementitious material by compound thermal activation. International Journal of Minerals, Metallurgy, and Materials, 16(3): 355-358.

[8] Liu Y., Du F., Yuan L., Zeng H., Kong S. F. (2010). Production of lightweight ceramisite from ironoretailings and its performance investigation in a biological aerated filter (BAF) reactor. Journal of Hazardous Materials, 178(1-3): 999-1006.

[9] Liu S. L. (2011): Application of cement filling inTieshan Iron Mine. Nonferrous Metals, 63(1): 5-7.

[10] Fall M., Benzaazoua M., Ouellet S. (2005): Experimental characterization of the influence of tailings fineness and density on the quality of cemented paste backfill. Minerals Engineering, 18, (1): 41-44.

[11] Kesimal A., Ercikdi B., Yilmaz E. (2003): The effect of desliming by sedimentation on paste backfill performance. Minerals Engineering, 16(10): 1009-1011.

[12] Zhang J. R., Ni W., Jia Q. M,. (2007): Investigation on making autoclaved tailing bricks from iron tailings in Tangshan District. Metal Mine, (3): 85-87.

[13] Jia Q. M., Zhang J. R., F. J. Li. (2006): Study on hige silicon iron tailing making tailing brick. China Mining Magazine, 15(4): 39-41.

[14] Zhao Y. L., Zhang Y. M., Chen T. J., Zhao Y. L., Bao S. X.. (2012): Preparation of high strength autoclaved bricks from hematite tailings. Constr Build Mater, 28(1): 450-455.

[15] Zhao Y. L., Zhang Y. M., Chen T. J. (2012): Effect of autoclaved schedule for compressive strength of hematite tailing bricks. Metal Mine, (5): 164-164.

[16] Oelkers E. H., Schott J. L., Devidal J. (1994): The effect of aluminum, pH, and chemical affinity on the rates of aluminosilicate dissolution reactions. Geochim Cosmochim Acta, 58(9): 2011-2024.

[17] Xiao Y., Lasaga A. C. (1994): Ab initio quantum mechanical studies of the kinetics and mechanism of silicate dissolution: H+(H3O+) catalysis. Geochim Cosmochim Acta, 58 (12): 5379-2024.

[18] Hellmann R., Darn J. C., Mea G. D. (1997): The albite-water system Part III. Characterization of leached and hydrogen-enriched layers formed at 300C using MeV ion beam techniques Geochim Cosmochim Acta, 61(8): 1575-1594.

[19] Coleman N. J., Brassington D. S. (2003): Synthesis of Al-substituted 11 Å tobermorite from newsprint recycling residue: A feasibility study. Mater Res Bull, 38(3): 485-497.

[20] Siauciunas R., Baltusnikas A. (2003): Influence of SiO2 modification on hydrogarnets formation during hydrothermal synthesis. Cement & Concrete Research, 33(10): 1789-1793.

[21] Fu K. R. (2006): The discussion of autoclaved aerated concrete curing system. New Build Mater, (12): 72-74.

[22] Fang Y. H., Pang E. B, Wang R., Xuan W., Chen Y. F. (2010). Aytoclaved sand-lime bricks from copper mine tailing with low SiO2 content. Journal of the Chinese Ceramic Society, 38(4): 559-563.

[23] Bensted J., Barnes P. (2002): Structure and performance of cements. 2nd edition. New York: Spon Press.